Journal of Taibah University for Science

ISSN: (Print) (Online) Journal homepage: https://www.tandfonline.com/loi/tusc20

Synthesis, characterization and solvatochromic behaviour of new water-soluble 8-hydroxy-3,6-disulphonaphthyl azohydroxynaphthalenes

Olusegun E. Thomas & Olajire A. Adegoke (Deceased)

To cite this article: Olusegun E. Thomas & Olajire A. Adegoke (Deceased) (2022) Synthesis, characterization and solvatochromic behaviour of new water-soluble 8-hydroxy-3,6-disulphonaphthyl azohydroxynaphthalenes, Journal of Taibah University for Science, 16:1, 451-462, DOI: 10.1080/16583655.2022.2070903

To link to this article: https://doi.org/10.1080/16583655.2022.2070903

Published online: 09 May 2022.

JOURNAL OF TAIBAH UNIVERSITY FOR SCIENCE
2022, VOL. 16, NO. 1, 451–462
https://doi.org/10.1080/16583655.2022.2070903

JTUSCI

Journal of Taibah University for Science

Taylor & Francis
Taylor & Francis Group

OPEN ACCESS Check for updates

Synthesis, characterization and solvatochromic behaviour of new water-soluble 8-hydroxy-3,6-disulphonaphthyl azohydroxynaphthalenes

Olusegun E. THOMAS and Olajire A. ADEGOKE (Deceased)

Department of Pharmaceutical Chemistry, University of Ibadan, Ibadan, Nigeria

ABSTRACT

A series of five tetracyclic mono azo dyes based on the diazotization of 1-amino-8-hydroxynaphthalene-3,6-disulphonic acid and subsequent coupling with substituted (un)sulphonated naphthalene derivatives have been synthesized. The chemical structures of the dyes were established using UV–visible, IR, NMR as well as mass spectrometry. Based on the number of sulphonic acid and other hydrophilic groups they contain, the compounds showed varying extent of water solubility. Spectroscopic characterization revealed the existence of azo-hydrazone tautomerism and the influence of the structures of solvating solvents on the equilibrium. Statistical analysis of single, dual and multiparametric equations of Kamlet Abboud and Taft parameters showed that solvent polarity was the most significant contributor to the observed spectral patterns of the dyes in pure solvents. The compounds could find useful applications as solvatochromic probes, food and drug colour additives.

ARTICLE HISTORY
Received 21 November 2021
Revised 1 April 2022
Accepted 23 April 2022

KEYWORDS
1-amino-8-hydroxynaphthalene-3,6-disulphonic acid; azo compounds; synthesis; spectroscopic characterization; azo-hydrazone tautomerism; solvatochromic properties

1. Introduction

Azo dyes are widely used in the textile, printing, plastics, cosmetics and food industries [1,2]. Of these industrial dyes, sulphonated azoaromatic compounds are the most commonly utilized. For example, nearly 70% of dyes employed in textile processing belong to this chemical class [3]. The number and position of sulphonic acid groups per azo molecule have been shown to have effects on their colour, solvatochromic properties and by extension their applications as photochromic or solvatochromic probes [4–6]. In addition, sulphonic acid group substitution in azoaromatic structures improves their water solubility. This increases both the applicability of the dyes in terms of application media, as well as the eco-friendly bacterial degradation of the dyes under certain conditions [7–9]. A prominent route of sulphonation involves the azo coupling of diazotized aromatic amines with naphthalene sulphonic acids, such as 1-amino-8-hydroxynaphthalene-3,6-disulphonic acid, which is perhaps the most commonly utilized dye intermediate in that regard [10]. 1-amino-8-hydroxynaphthalene-3,6-disulphonic acid has therefore been employed as a coupling component in the synthesis of azo dyes of varying functionality [11,12]. Chemically, 1-amino-8-hydroxynaphthalene-3,6-disulphonic acid contains free hydroxyl and amino groups, each of which can dictate the position of electrophilic aromatic substitution by an incoming diazonium ion during coupling reactions. Consequently, diazo coupling to 1-amino-8-hydroxynaphthalene-3,6-disulphonic acid can occur at *para* positions to either its free hydroxyl or amino groups in alkaline or acidic pH respectively.

Nevertheless, both coupling reaction conditions will yield azo products with sulphonic groups at *ortho* position to the azo linkage. This chemical feature might be undesirable in certain instances such as the reported reduced ability of aerobic azo reductase from *Xenophilus azovorans* to degrade *ortho* sulpho azo compounds [13]. The alternative use of 1-amino-8-hydroxynaphthalene-3,6-disulphonic acid as an amine precursor for diazotization will therefore provide more options as to the chemical structures that can be incorporated into 1-amino-8-hydroxynaphthalene-3,6-disulphonic acid derived dyes. In particular, it will provide an additional chemical route to preclude having a sulphonic acid group at *ortho* position to the azo linkage in this series of compounds. However, to the best of our knowledge, little or no report exists as regards the diazotization of 1-amino-8-hydroxynaphthalene-3,6-disulphonic acid and its use as a diazonium ion precursor in the synthesis of azo compounds. This might partly be due to its poor solubility in mineral acids. The objective of the study was therefore to successfully diazotize 1-amino-8-hydroxynaphthalene-3,6-disulphonic acid and couple it with hydroxynaphthalenes residues to afford new tetracyclic azo compounds containing two to four sulphonic acid groups per dye molecule.

CONTACT Olusegun E. THOMAS seguntom@yahoo.com Department of Pharmaceutical Chemistry, University of Ibadan, Orita UI, Ibadan 200284, Nigeria

2. Experimental

2.1. Materials

1-amino-8-hydroxynaphthalene-3,6-disulphonic acid monosodium salt (Sigma Aldrich), 1-amino-8-naphthol-4-sulphonic acid (TCI), 7-amino-4-hydroxyl-2-naphth alenesulphonic acid J-acid (Fluka Analytical), silica gel GF_{254} (precoated aluminium sheets, Merck Germany). All the other reagents and solvents were sourced from BDH UK and used without additional purification. Double distilled water was used for the preparation of all solutions.

2.2. Instrumentation

Mettler analytical balance (Ohaus Pioneer, New Jersey), melting point apparatus (Stuart England), ultrasonic water bath (Langford UK), magnetic stirrer (Gallenkamp UK), UV–visible spectrophotometer (Perkin Elmer Lambda 25, Massachusetts), IR spectrophotometer (Perkin Elmer Spectrum BX), nuclear magnetic resonance spectrometer (Bruker DPX 300 and 500 MHz, Billerica), mass spectrometer (QTof Micro Micromass, Milford).

2.3. Synthesis

2.3.1. General procedure for synthesis of 8-hydroxy-3,6-disulphonaphthalene-1-diazonium (1)

A mixture of 1-amino-8-hydroxynaphthalene-3,6-disulphonic acid monosodium salt (0.10 g, 0.30 mmol) dissolved in 10 mL of 0.5% w/v aqueous $NaHCO_3$ and 2 mL aqueous solution of Na_2SO_4 (0.02 g, 0.14 mmol) were continuously stirred at 0°C as a cold aqueous solution of $NaNO_2$ (0.3 g, 4.35 mmol) was added dropwise over 10 min. After stirring for an additional 10 min, the resultant solution was added drop by drop to a continuously stirred 10 mL solution of 1M HCl maintained at 0°C. The reaction mixture was covered with aluminium foil and allowed to proceed for 90 min at 0°C after which urea (2.5 g, 42.0 mmol) was added. The resultant golden yellow diazonium solution (**1**) was used without isolation.

2.3.2. General procedure for the synthesis of 8-hydroxy-3,6-disulphonaphthyl azohydroxynaphthalenes (3a–e)

A batch of 8-hydroxy-3,6-disulphonaphthalene-1-dia zonium (**1**) as prepared in 2.3.1 was added dropwise into continuously stirred solutions of substituted naphthol compounds (**2a–e**) (0.30 mmol) in optimized coupling solutions as depicted in Table 1. In each case, the reaction was stirred for 3 h at 0°C and the progress monitored with TLC. The TLC conditions employed included silica gel stationary phase with the following mobile phases, butanol:ethanol:water:25% ammonia (3:3:1:1); methanol:N,N-dimethylformamide:ethyl acetate (5:2:3); ethyl acetate:1-propanol:ethanol:25% ammonia (4:1:4:1) and reversed-phase silica with 40% aqueous methanolic solution as mobile phase. After completion of the reaction, the reaction mixture was acidified (pH 1–2) with concentrated HCl and sufficient sodium chloride added to precipitate out the compound. The crude product was collected by filtration and dried at 70°C. The product was re-dissolved in 50 mL water and filtered, after which a sufficient amount of sodium chloride was added to the filtrate to initiate salting out of the dye. The mixture was allowed to stand overnight at 4°C before the product was collected by filtration.

Final recrystallization was done by refluxing using the optimized solvents and conditions as depicted in Table 1 before the solid products (**3a–e**) were collected by filtration and dried at 70°C.

The NMR spectra of the compounds (**3a–e**) were recorded at room temperature in DMSO-d_6 solutions and their chemical shifts with respect to residual protons of the solvent are given below.

4-hydroxy-5-[(1E)-2-(4-hydroxynaphthalen-1-yl)dia zen-1-yl]naphthalene-2,7-disulphonic acid **(3a)**

Colour: Violet; mp:270–275°C Yield: 65.3%; IR (KBr) cm^{-1} = 3442.26 (OH), 1397.30 (N = N), 1190.25 (C–O); ^{1}H NMR (DMSO-d_6 500 MHz) δ : 8.83 (s, 1H), 8.26 (m, J = 7.62 Hz, 1H), 8.10 (s, 2H), 7.94 (m, 1H), 7.86 (s, 1H), 7.83 (m, J = 7.62 Hz, 1H), 7.63 (m, J = 7.83 Hz, 1H), 7.55 (s, 1H), 7.17 (m, J = 7.83 Hz, 1H), 7.08 (s, 1H), 6.70 (d, 1H), 6.65 (s, 1H), 6.38 (s, 1H Hydroxyl), 4.76 (s, 1H); ^{13}C NMR (DMSO-d_6 300 MHz) δ : 106.0 (C-6), 109.56 (C-15), 110.66 (C-8), 113.57 (C-2), 114.5 (C-4), 114.9 (C-13), 116.8 (C-12), 122.5 (C-10), 122.65 (C-19), 123.54 (C-16), 124.0

Table 1. Optimized procedures for the synthesis of 8-hydroxy-3,6-disulphonaphthyl azohydroxynaphthalenes **(3a–e).**

Dye	Substituted naphthol	Optimized coupling solutions	Final recrystallization	Yield[a] (%)
3a	1-naphthol	50 mL 0.5M NaOH	Reflux in ethanol	65.3
3b	2-naphthol	50 mL 0.5M NaOH	Reflux in ethanol	69.4
3c	1-amino-8-hydroxynaphthalene-3,6-disulphonic acid	60 mL aqueous solution of Na_2CO_3 (15 mmol,) and $NaHCO_3$ (9.57 mmol)	Reflux in DMF then precipitation with acetone	74.9
3d	7-amino-4-hydroxyl-2-naphthalenesulphonic acid	60 mL aqueous solution of Na_2CO_3 (15 mmol,) and $NaHCO_3$ (9.57 mmol)	Reflux in methanol then precipitation with diethyl ether	48.5
3e	1-amino-8-naphthol-4-sulphonic acid	60 mL aqueous solution of Na_2CO_3 (15 mmol,) and $NaHCO_3$ (9.57 mmol)	Methanol/ethyl acetate (45:55, v/v) binary solvent at room temperature	47.1

[a]Yield refers to isolated pure compound.

(C-17), 129.59 (C-18), 135.12 (C-5), 135.33 (C-3), 138.0 (C-20), 142.5 (C-11), 146.57 (C-1), 147.75 (C-7), 153.58 (C-9), 155.16 (C-14); Negative-ion ESI: *m/z* 473.0 ([M–H]$^-$). Calculated *M* 474.01.

4-hydroxy-5-[(1E)-2-(2-hydroxynaphthalen-1-yl)diazen-1-yl]naphthalene-2,7-disulphonic acid **(3b)**

Colour: Blue; mp: 277°C Yield: 69.4%; IR (KBr) cm^{-1}: 3443.75 (NH), 1621.58 (C = O), 1476.92 (C = N), 1192.43 (C–O); ^{1}H NMR (DMSO-d_6 500 MHz) δ : 11.70 (s, 0.88H hydrazone NH), 9.86 (s, 0.11H azo OH), 8.45 (s, 1H), 8.38 (d, J = 8.0 Hz, 1H), 7.94 (s, 1H), 7.89 (d, J = 9.5 Hz, 1H), 7.72 (d, J = 8.0 Hz, 1H), 7.65 (t, J = 7.5 Hz, 1H), 7.63, 7.45 (t, J = 7.5 Hz, 1H), 7.28 (s, 1H), 6.71 (d, J = 9.5 Hz, 1H), 5.47 (s, 5H); ^{13}C NMR (DMSO-d_6 300 MHz) δ : 108.56 (C-8), 109.75 (C-4), 114.63 (C-10), 116.50 (C-2), 121.43 (C-6), 122.62 (C-16), 126.63 (C-13), 126.78 (C-17), 128.09 (C-5), 129.37 (C-18), 129.5 (C-19), 130.23 (C-20), 133.5 (C-15), 135.06 (C-7), 139.54 (C-3), 141.92 (C-14), 146.69 (C-1), 153.38 (C-9), 160.11 (C-11), 177.71 (C-12); Negative-ion ESI: *m/z* 473.0 ([M–H]$^-$). Calculated *M* 474.01.

5-amino-4-hydroxy-1-[(1E)-2-(8-hydroxy-3,6-disulphonaphthalen-1-yl)diazen-1-yl]naphthalene-2,7-disulphonic acid **(3c)**

Colour: Purple; mp: 310–312°C; Yield: 74.9%; IR (KBr) cm^{-1}: 3447.0 (NH), 1635.48 (C = O), 1482.10 (C = N), 1195.38 (C–O); ^{1}H NMR (DMSO-d_6 500 MHz) δ :16.43 (s, 0.7H hydrazone NH), 11.47 (s, 1H), 10.49 (s, 1H), 8.52 (s, 1H), 7.81 (s, 1H), 7.62 (s, 1H), 7.34 (s, 1H), 7.23 (s, 1H), 7.11 (s, 1H), 7.07 (s, 2H), 6.99 (s, 0.84H), 6.93 (s, 1H), 5.46 (s, 0.3H Azo OH), 2.51 (s, 2H); ^{13}C NMR (DMSO-d_6 300 MHz) δ : 108.21 (C-8), 109.99 (C-2), 112.27 (C-13), 113.66 (C-17), 114.19 (C-10), 114.19 (C-15), 116.47 (C-6), 120.76 (C-4), 123.64 (C-19), 126.1 (C-5), 129.77 (C-20), 134.91 (C-3), 135.15 (C-7), 136.22 (C-11), 139.83 (C-1), 142.23 (C-18), 145.92 (C-12), 146.54 (C-16), 153.25 (C-9), 180.71 (C-14); Negative-ion ESI: *m/z* 669.82 ([M – 2H + Na]$^-$). Calculated *M* 671.59 (monosodium salt)

4-[(1E)-2-(7-amino-4-hydroxy-2-sulphonaphthalen-1-yl)diazen-1-yl]-5-hydroxynaphthalene-2,7- disulphonic acid **(3d)**

Colour: Magenta; mp: 300–305°C, Yield: 48.5%; IR (KBr) cm^{-1}: 3440.12 (NH), 1616.0 (C = O), 1482.75 (C = N), 1194.42 (C–O); ^{1}H NMR (DMSO-d_6 500 MHz) δ : 16.78 (s, 1H hydrazone NH), 8.43 (s, 2H), 7.92 (d, J = 8.5 Hz, 2H), 7.81 (s, 1H), 7.61 (s, 1H), 7.34 (s, 1H), 7.20 (s, 1H), 6.71 (d, J = 8.5 Hz, 1H), 6.68 (s, 1H), 6.38 (s, 2H), 5.74 (s, 2H); ^{13}C NMR (DMSO-d_6 300 MHz) δ :108.81 (C-8), 109.39 (C-2), 110.66 (C-19), 114.24 (C-10), 114.5 (C-17), 116.29 (C-6), 120.21 (C-15), 120.84 (C-4), 122.84 (C-13), 129.4 (C-16), 129.52 (C-20), 134.87 (C-5), 137.61 (C-7), 139.97 (C-18), 142.7 (C-12), 145.61 (C-11), 146.61 (C-1), 153.4 (C-9), 159.82 (C-3), 176.77 (C-14); Negative-ion ESI: *m/z* 590.94 ([M–2H + Na]$^-$). Calculated *M* 591.53 (monosodium salt)

4-[(1E)-2-(5-amino-4-hydroxy-8-sulphonaphthalen-1-yl)diazen-1-yl]-5-hydroxynaphthalene-2,7-disulphonic acid **(3e)**

Colour: Blue; mp:300–305°C, Yield: 47.1%; IR (KBr) cm^{-1}: 3435.40 (NH), 1624.87 (C = O), 1487.82 (C = N), 1188.96 (C–O); ^{1}H NMR (DMSO-d_6 500 MHz) δ : 11.53 (s, 1H hydrazone NH), 8.23 (s, 1H), 7.94 (d, J = 9.9 Hz, 1H), 7.79 (d, J = 8.7 Hz, 1H), 7.76 (s, 1H), 7.56 (s, 1H), 7.2 (s, 1H), 6.96 (d, J = 9.9 Hz, 1H), 6.60 (d, J = 8.7 Hz, 1H), 5.48 (s, 2H); ^{13}C NMR (DMSO-d_6 300 MHz) δ :108.19 (C-2), 108.41 (C-8), 112.4 (C-13), 112.77 (C-15), 113.1 (C-20), 114.06 (C-10), 116.44 (C-6), 121.0 (C-4), 122.58 (C-18), 127.44 (C-17), 133.2 (C-5), 133.73 (C-12), 134.45 (C-19), 135.01 (C-11), 139.11 (C-16), 146.32 (C-3), 146.56 (C-7), 149.16 (C-1), 159.95 (C-9), 181.10 (C-14); Negative-ion ESI: *m/z* 586.74 ([M–2H + Na]$^-$). Calculated *M* 591.53 (monosodium salt)

2.4. Solvatochromic assessment

The UV–visible spectra of the dyes dissolved at 1.44 – 2.01 × 10^{-5}*M* concentrations in neat organic solvents were acquired at 25°C.

3. Results and discussion

The overall reaction and structures of the five new tetracyclic azo compounds are shown in Scheme 1. The optimized reaction conditions for synthesis are indicated in Table 1.

3.1. Water solubility

The water solubility of the compounds increased with the number of sulphonic acid groups per dye molecule. Thus, water solubility increased from disulphonated **3a** and **3b** (10 and 14 mg/10 mL respectively), trisulphonated **3d** and **3e** (20 mg/mL) to tetrasulphonated **3c** (40 mg/mL). The sulphonic acid group improves water solubility *via* ion-dipole interactions and by its ability to serve as both hydrogen bond donors and acceptors [14]. Hydroxyl and amino groups, which are also present in the compounds, have been estimated to possess carbon-solubilizing potential of five to seven carbon atoms each [15]. An organic molecule becomes water-soluble when the combined solubilizing potential of the functional groups present in it exceeds the total number of carbon atoms it contains. The enhanced water solubility of the synthesized dyes can increase their applicability in textile and printing industries. More importantly, the combination of high water solubility, extreme polarity and high molecular weights will hinder lipophilicity, bioaccumulation and consequently reduce the toxicity of the compounds [16]. These are particularly critical attributes for clinical marker dyes or food/drug colour additives that are not expected to reach systemic circulation. It is noteworthy that the most commonly used food and drug additives such as amaranth, tartrazine, and sunset yellow all contain varying number of sulphonic acid groups [17].

3.2. Azo-hydrazone tautomerism

The five compounds, **3a–e**, are capable of forming hydrazone tautomers as depicted in Scheme 2. However, formation of the hydrazone of **3b**, which is an *ortho* hydroxyl azo compound, involves the intramolecular rearrangement of the *ortho* hydroxyl group with the azo linkage in such a manner that an extra cyclic structure is formed [18]. The proton is therefore unavailable for intermolecular interactions. On the other hand, the formation of hydrazone tautomers of **3a, 3c, 3d** and **3e** involves the *para* hydroxyl group, which is labile and available for interactions with solvent milieu [19]. Nevertheless, the predominance of both types of hydrazone tautomers is associated with the formation of the ketonic group as shown in Scheme 2. The azo-hydrazone tautomerism of **3a–e** was therefore investigated using IR, NMR and UV–visible spectroscopy.

3.2.1. IR spectroscopic analyses

The stretching vibrations of νN = N linkage are typically found at 1400–1450 cm^{-1} [20]. Consequently, only the band at 1397.30 cm^{-1} in IR spectra of **3a** could be attributed to azo tautomeric form. On the contrary, FT-IR spectra of **3b–e** revealed medium absorption bands located at 1476.92 cm^{-1} (**3b**), 1482.10 cm^{-1} (**3c**), 1487.75 cm^{-1} (**3d**) and 1487.82 cm^{-1} (**3e**) which were assigned to the νC = N vibrations of their hydrazone tautomers [18]. The sharp bands located around 1616.0 and 1635.48 cm^{-1} were mainly assigned to νC = O vibrations. A similar frequency range of 1620–1635 cm^{-1} was obtained with the νC = O vibrations of hydrazone tautomers of a series of twelve arylazonaphthols [21]. The νmax values at 1188.96–1195.35 cm^{-1} were assigned to νS = O of sulphonic acids and νC–O bonds.

3.2.2. ^{1}H and ^{13}C NMR characterization of azo-hydrazone tautomerization

The ^{13}C NMR shifts of azo forms are usually found around 160 ppm due to the carbon bearing the hydroxyl while chemical shifts of hydrazone forms are routinely found around 170 ppm due to the formation of the ketonic group [18,22]. The ^{13}C NMR spectra of the five dyes are depicted in Figure 1. The spectra of **3b–e** revealed low field chemical shifts which correspond to the ketonic group. Consequently, the peak at 177.71 ppm was assigned to C12 in **3b** while the chemical shifts of 180.71, 176.77 and 181.10 ppm were assigned to C14 of **3c**, **3d** and **3e** respectively.

This confirmed that **3b–e** exist predominantly as the hydrazone tautomers. However, no peak at such low field could be observed in ^{13}C NMR of **3a**, which is suggestive, the compound exists majorly in the azo form. The chemical shifts of the protons of the naphthalene rings of the five compounds can be easily assigned as they occur in the aromatic region and by using the splitting patterns as shown in Figure 2. Hydrazone formation is also associated with low field peaks in ^{1}HNMR [18]. As depicted in the representative ^{1}HNMR of **3c** and **3d**, the active peaks found at 16.431 and 16.788 ppm and with an integral height of 0.71 and 1.0 respectively were therefore attributed to the N–H bonds of the hydrazone form of the compounds (Figure 3). We have also attributed the peak in ^{1}HNMR of **3c** found at 5.467 ppm and with an integral height of 0.3 to its azo form. Thus the hydrazone tautomeric ratios of **3c** and **3d,** calculated from the peak heights, are 71% and 100% respectively. The predominance of the hydrazone forms of **3c** and **3d** is anticipated as the presence of electron-withdrawing sulpho groups at *meta* position to C-14 hydroxyl group (Scheme 2) increases its propensity for proton release and the subsequent formation of the ketonic group [23]. The increased azo ratio of **3a** could therefore be attributed to its lack of electron-withdrawing groups. The most deshielded protons in the ^{1}HNMR of **3b and 3e** were found at 11.703 and 11.528 ppm respectively and were therefore assigned to the NH of their hydrazone tautomers. The peaks with the respective integral of 0.88 and 1.0 confirmed that both compounds exist majorly in the hydrazone form.

3.2.3. pH-driven azo-hydrazone tautomerism

The UV–visible spectra of aqueous solutions of the compounds at concentrations of 2.11×10^{-5} (**3a** and **3b**), 1.48×10^{-5} (**3c**) and 1.69×10^{-5} (**3d** and **3e**) were acquired at room temperature. The effect of pH on the azo-hydrazone equilibrium of the compounds was investigated by the addition of various volumes of 2 M HCl or NaOH to the solutions of the dyes. The results are depicted in Figure 4. An aqueous solution of **3a** has a pH of 6.80 and 3 UV–vis absorption bands. The absorption bands at 351 and 546 nm are due to $\pi - \pi^*$ transition of its hydrazone form [18,24]. A decrease in pH from 6.8 to 3.1 will lead to a shift of the equilibrium towards imino or hydrazone formation. This is associated with a loss of conjugation as depicted in Scheme 2. Expectedly, a large hypsochromic shift ($\Delta\lambda_{max} = 40$ nm) was observed with a decrease in pH. On the other hand, the addition of NaOH to the neutral solution of **3a** produced a maximum bathochromic shift of $\Delta\lambda_{max} = 10$ nm only as the compound already exists majorly in azo form. This, therefore, agrees with NMR data that **3a** exists predominantly in the azo tautomeric form.

The pH of an aqueous solution of **3b** is 6.8 and its UV–visible spectra showed three bands at 225, 297 and 513 nm with the latter two ascribed to the $\pi - \pi^*$ transition of the hydrazone tautomer. As deduced from the NMR data, **3b** exists predominantly in the hydrazone form in which the imino group is protonated. Expectedly, the addition of HCl did not change the position of the 513 nm band. However, when pH increased from 6.8 to 10.48, the peaks at 297 and 513 nm disappeared and in their stead, two new red-shifted peaks

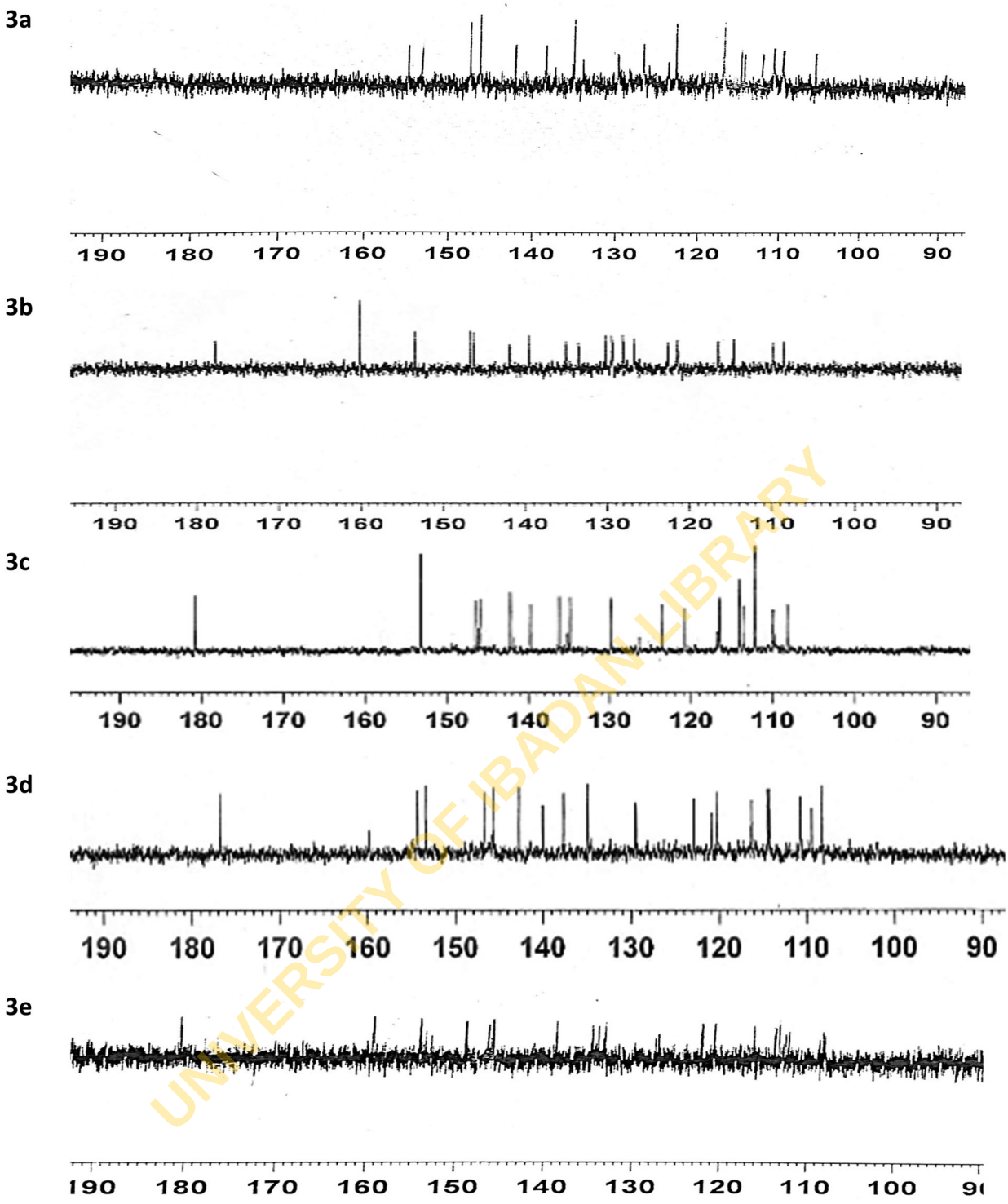

Figure 1. ^{13}C NMR peaks of **3a–e** in DMSO-d_6.

could be observed at 308 and 544 nm respectively. In addition, a new band at 379 nm was seen with the increase in pH. The bathochromic shifts are suggestive of a shift of equilibrium towards azo formation and the naphtholate anion. The increased electron density of the azo linkage and naphtholate anion will lead to increased conjugation and the observed bathochromic shifts [14]. Similarly, the addition of HCl to aqueous solutions of **3c**, **3d** and **3e** did not induce any shift in the position of its bands but on the contrary, increase in pH produced bathochromic shifts of $\Delta\lambda_{max} = 20$ nm, $\Delta\lambda_{max} = 31$ nm and $\Delta\lambda_{max} = 22$ nm respectively. Thus, it can be concluded that the hydrazone form of **3c**, **3d** and **3e** dominate in neutral and acidic conditions as suggested by NMR data [25].

3.3. Solvatochromism of dyes

The various colours exhibited by the dyes when introduced into neat organic solvents are depicted in Table 2. The representative electronic absorption spectra of the five dyes in selected solvents: ethanol, acetonitrile,

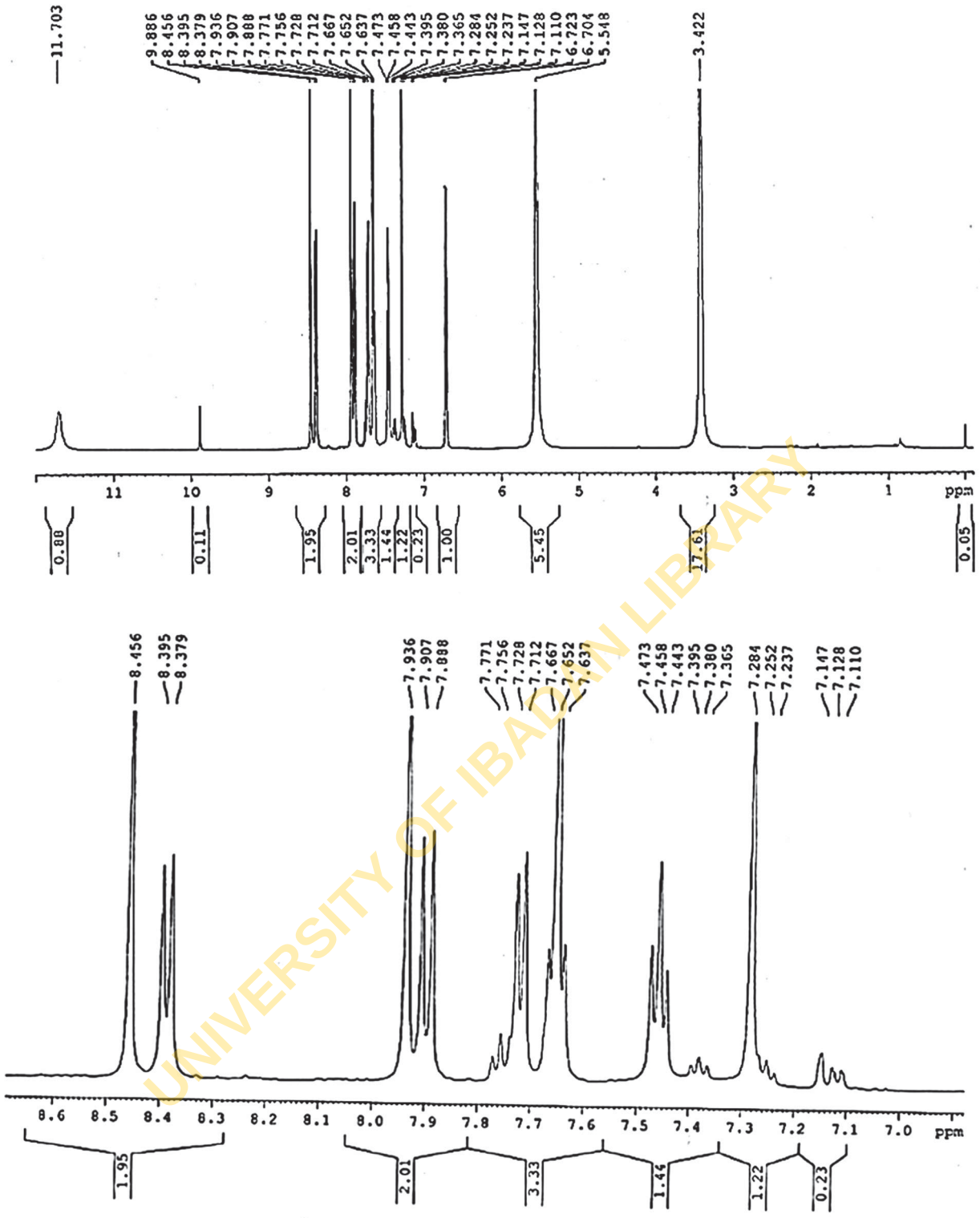

Figure 2. Peak splits in the aromatic protons of **3b**.

acetone, ethyl acetate and DMF are shown in Figure 5(a–e) respectively.

The high-energy bands consisted of high-intensity peaks at around 230–259 nm and relatively less intense bands with peaks in the range of 292–314 nm. The high-energy absorption bands were due to the $\pi-\pi*$ transitions of the aromatic naphthalene residues. The positions of the low-energy absorption bands (which arises from the $\pi-\pi^*$electronic transitions of interactions between azo chromophoric units and surrounding solvent molecules) varied from 460 to 592 nm and bore a relationship with the chemical structures of the solutes, solvents characteristics and the predominant solute-solvent interactions including non-specific (polarity) and specific (intermolecular) interactions at play. The variation of the molar transition energies

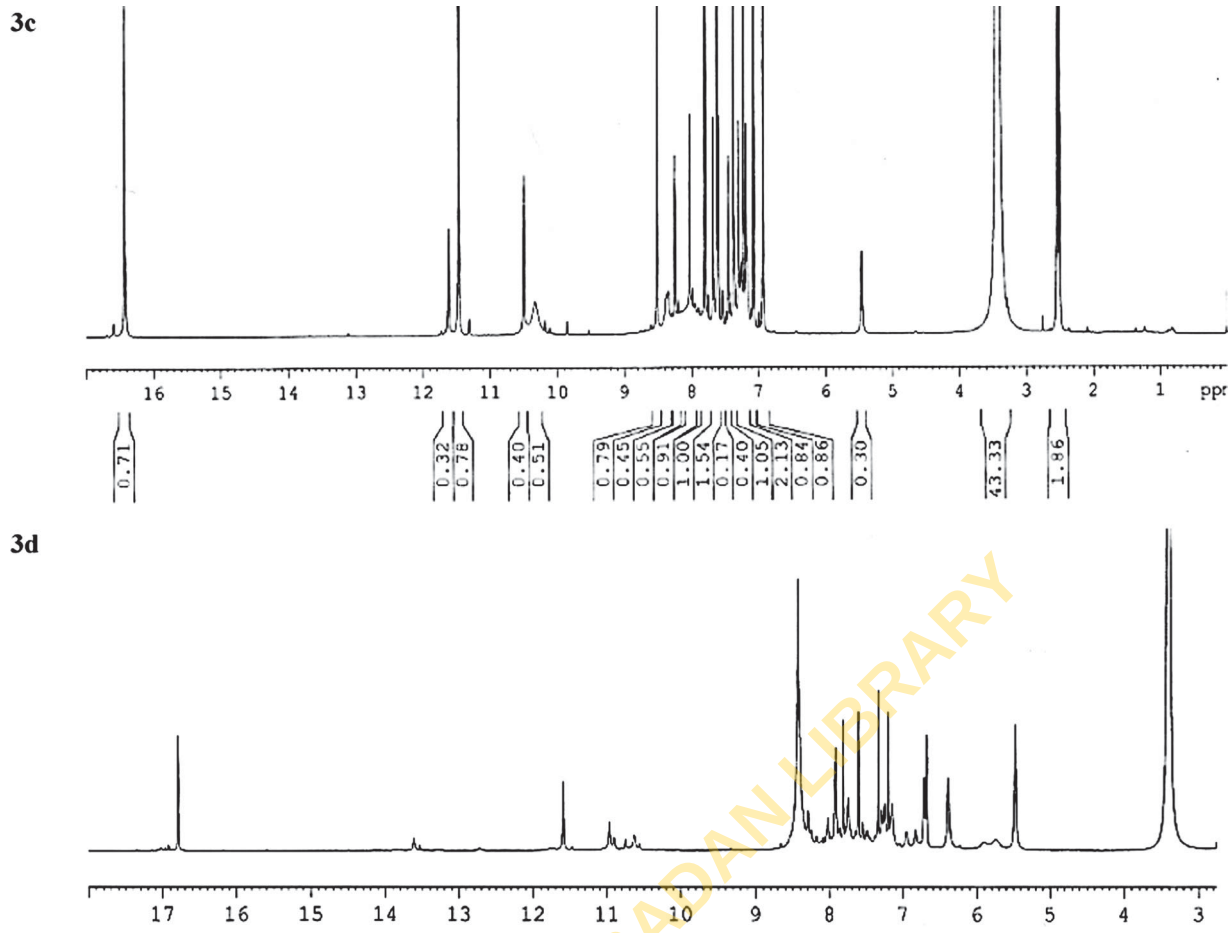

Figure 3. ^{1}H NMR of **3c** and **3d** showing highly deshielded protons of the hydrazone tautomers.

Table 2. Colours of the dyes in various solvents.

Compound	Methanol	1,4-dioxane	Acetonitrile	DMF	Ethyl acetate	Methanol + 1M HCl	Methanol + 1M NaOH
3a	Pink	Pink	Red	Blue	Brown	Orange	Purple
3b	Pink	Pink	Pink	Pink	Brown	Pink	Pink
3c	Purple	Magenta	Magenta	Purple	Brown	Magenta	Magenta
3d	Orange	Orange	Peach	Pink	Brown	Orange	Purple
3e	Purple	Purple	Purple	Violet	Yellow	Purple	Indigo

of the compounds with the Kamlet, Abboud and Taft (KAT) parameters of solvents are depicted in Table 3.

With respect to ethyl acetate, progressive batho chromic shifts of $\Delta\lambda_{max} = 23$ nm, $\Delta\lambda_{max} = 39$ nm, and $\Delta\lambda_{max} = 79$ nm can be observed in the visible bands of **3a** as the solvent polarity increased from dioxane (π =0.48), propan-1-ol (π =0.52) to water (π =1.09). Similar increase in the positions of the visible bands was observed in the spectral patterns of the other dyes. This type of non-specific interaction is found when the excited state of a solute is better stabilized than the ground state in polar solvents. However, a cursory examination of the spectra data of **3a** in DMF and DMSO revealed higher bathochromic shifts than what was obtained in water despite its higher polarity. In contrast, no such bathochromic shifts were observed in the spectra of **3b** in either proton acceptor solvents. This is suggestive that a second or alternative solute-solvent interaction (other than polarity effects) was at play when solvated in DMF or DMSO [5]. Azo form is stabilized in hydrogen bond acceptor solvents while the basic imino group of the hydrazone form is stabilized in proton donating solvents [26]. Thus, when compared with **3b**, pronounced bathochromic shifts and hyperchromic changes were observed in the visible bands of **3a**, due to the availability of its C14 proton for hydrogen bond donation to DMF or DMSO. Similar bathochromic shifts were also observed in the spectra of **3c** and **3e** both of which contain free labile C14 proton available for donation to DMF. In addition, only a single visible band was observable in the electronic absorption spectra of **3b** while two visible bands were present in the spectra of **3a** when examined in both hydrogen bond acceptor solvents. Azo compounds such as **3b** that contain hydroxyl groups at *ortho* position to their azo bonds have been reported to exhibit a lone visible spectral band because of the involvement of the proton

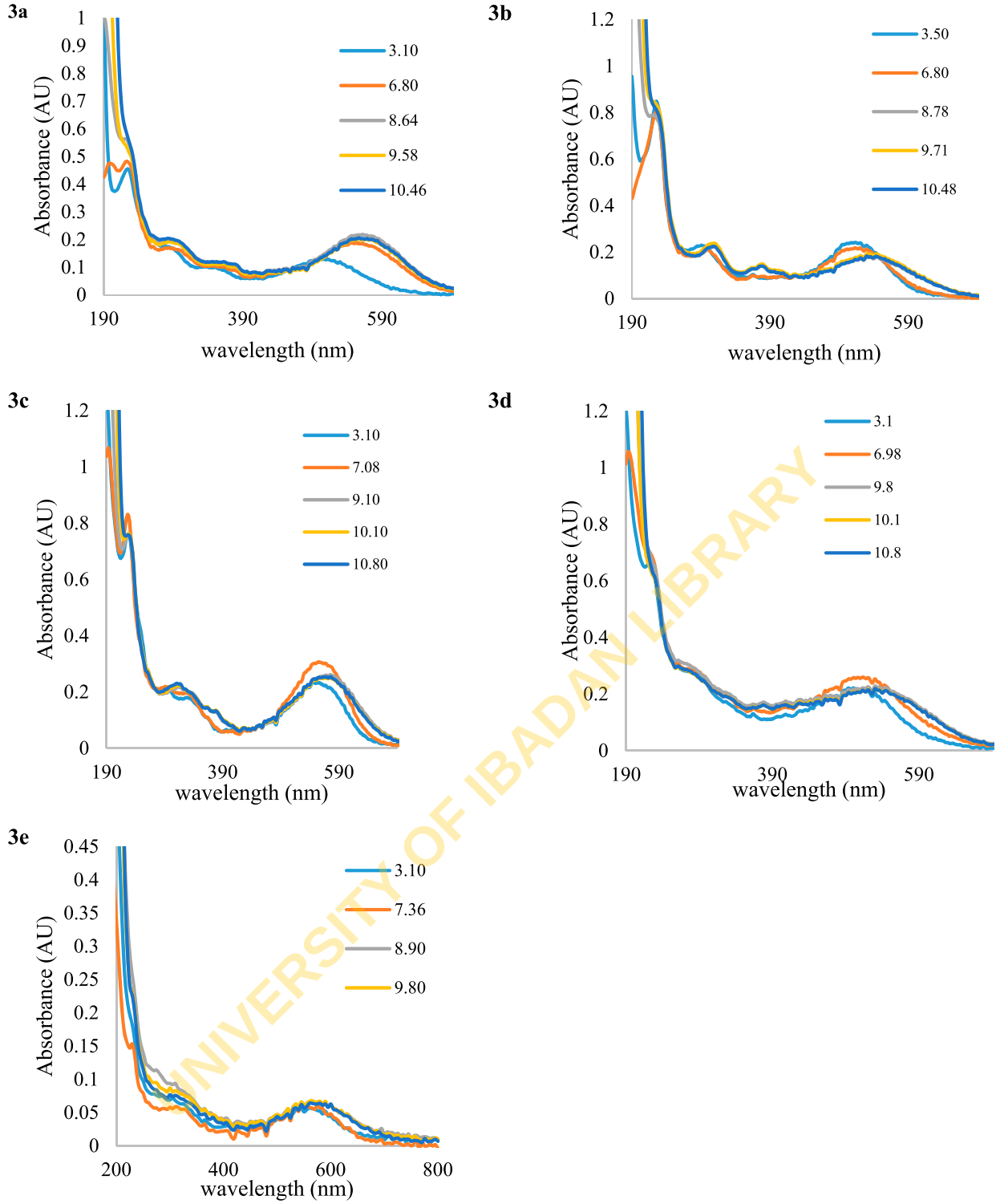

Figure 4. Effect of pH on azo-hydrazone tautomers of **3a–e** at $1.48 - 2.11 \times 10^{-5}$ concentrations.

in hydrazone formation and its consequent unavailability for solute-solvent interactions [5]. On the other hand, when present at *para* position to the azo linkages, azo-hydrazone equilibrium is more pronouncedly influenced by external environment including solute-solvent interactions [23], concentrations of co-solutes [27,28], charge and surfactant action [29]. For example, azo-hydrazone switching and consequent changes in the non-linear optical properties of methyl red were reported with increasing concentrations of amino acids and ionic surfactants [27].

The optical band gap energy associated with transition in the visible region of the compounds were determined from Tauc's plots using Equation (1):

$$\alpha.hv = A(hv - E_g)^n \quad (1)$$

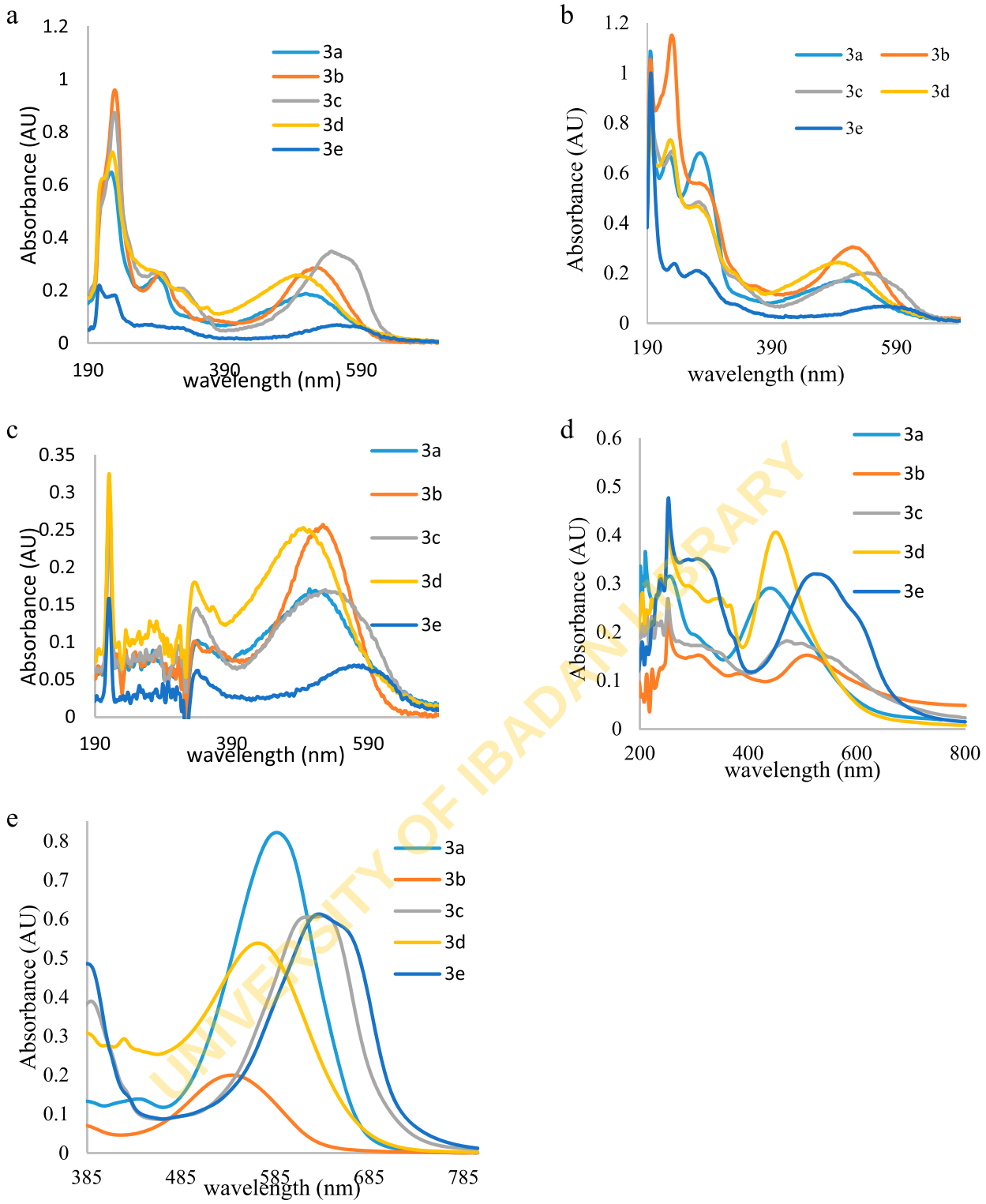

Figure 5. Electronic absorption spectra of the five dyes in (a) ethanol, (b) acetonitrile, (c) acetone, (d) ethyl acetate, (e) DMF at $1.44 - 2.01 \times 10^{-5}$***M*** concentrations.

where *hv* is the photon energy, E_g is optical energy gap, *A* is a constant that depends on transition probability while *n* can take up values of $\frac{1}{2}$, 2, 3/2 and 3 for direct allowed, indirect allowed, direct forbidden and indirect forbidden transitions respectively [30]. The four power probabilities were plotted against *hv* and the plot in which $n = \frac{1}{2}$ was found to best satisfy the lineal condition at the absorption edge. The optical energy gap of the compounds in organic solvents was determined by extrapolating the linear ascending part of the absorption edge to the *x*-axis of the Tauc's plots. Representative plots of compounds **3a–e** in acetone and ethyl acetate are depicted in Figure 6(a and b) respectively. The results showed that a change in solvent milieu from ethyl acetate to acetone led to an increase in the optical energy gap of **3b**, **3c** and **3e**. These compounds also

Table 3. Variation of the molar transition energies of the dyes with Kamlet–Taft parameters of solvents.

	E_T(log ε)					KAT parameters		
Solvent	3a	3b	3c	3d	3e	α	β	π^*
Acetone	55.30(3.94)	54.36(3.61)	53.44(4.19)	60.57(4.25)	51.89(4.20)	0.08	0.48	0.62
Acetonitrile	56.95(4.01)	54.56(3.72)	53.05(4.23)	60.83(4.12)	51.24(4.17)	0.19	0.40	0.66
1-Propanol	54.67(4.05)	54.15(3.73)	59.56(3.93)	59.69(4.19)	51.89(4.28)	0.84	0.9	0.52
2-Propanol	55.52(4.05)	54.36(3.75)	53.14(4.23)	59.19(4.16)	51.89(4.26)	0.76	0.81	0.48
Ethanol	56.07(4.07)	54.46(3.76)	52.65(4.35)	59.31(4.20)	51.89(4.24)	0.86	0.75	0.54
Methanol	56.62(4.05)	55.19(3.67)	52.46(4.34)	57.88(4.19)	51.89(4.24)	0.98	0.66	0.60
1,4-dioxane	56.40(3.97)	54.56(3.66)	52.37(4.20)	59.93(4.19)	51.33(4.16)	0.00	0.37	0.49
DMF	48.79(4.31)	53.44(3.69)	49.38(4.32)	56.17(4.20)	49.90(4.26)	0.00	0.69	0.88
DMSO	48.30(4.36)	53.84(3.73)	51.33(4.30)	56.06(4.11)	49.90(4.26)	0.00	0.76	1.00
Toluene	56.28(4.07)	54.67(3.75)	53.04(4.17)	60.57(3.95)	52.08(4.28)	0.00	0.11	0.49
Chloroform	59.57(3.82)	58.83(3.57)	58.11(3.61)	61.89(3.92)	53.34(3.72)	0.20	0.10	0.69
Ethyl acetate	59.07(4.16)	56.28(3.88)	60.70(4.10)	63.54(4.38)	54.88(4.28)	0.00	0.45	0.45
Dichloromethane	59.94(3.91)	58.35(3.47)	57.18(3.68)	62.15(4.06)	53.24(3.98)	0.13	0.10	0.73
Water	50.78(3.81)	53.44(3.54)	51.15(4.25)	55.41(4.09)	51.42(3.65)	1.17	0.47	1.09

E_T = molar transition energies of dyes; ϵ = molar absorption coefficients.

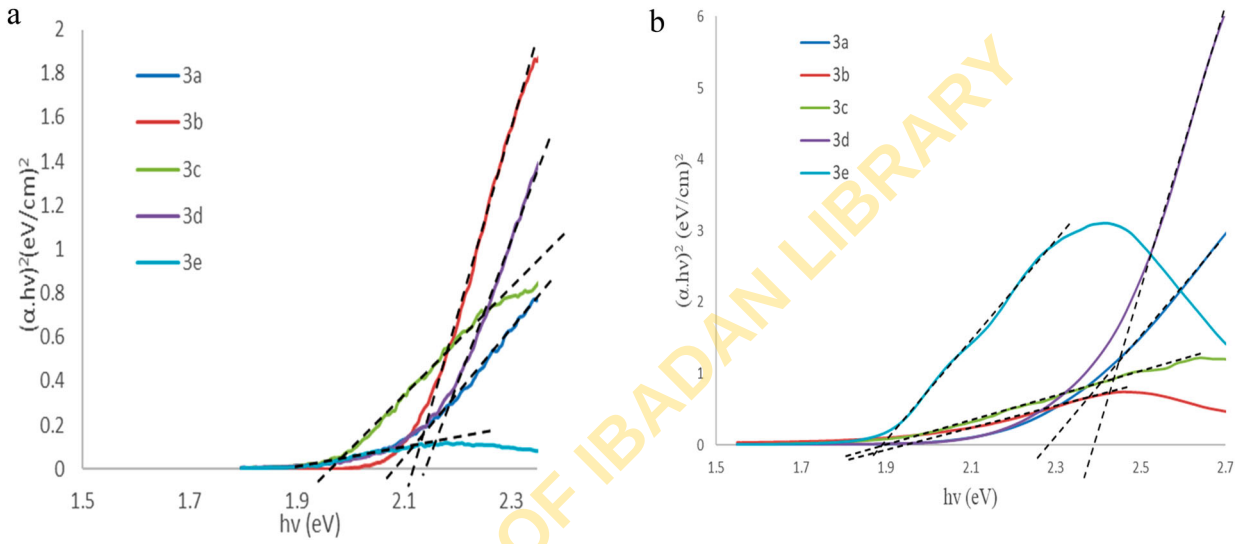

Figure 6. Tauc's plots of **3a–e** in (a) acetone and (b) ethyl acetate.

showed the lowest band gap in the solvents and are thus most suitable for optoelectronic devices [30].

3.4. Multiparametric correlation studies

In non-chlorinated solvents, the contributory roles of specific and non-specific interactions to the total molar transition energies of a solute can be estimated by single, dual and multiparametric statistical analysis of Equation (2).

$$E_T = A_\circ + a\alpha + b\beta + p\pi^* \quad (2)$$

where $A_\circ$ is the intercept of the regression equation, *a*, *b* and *p* are the regression coefficients that measure the

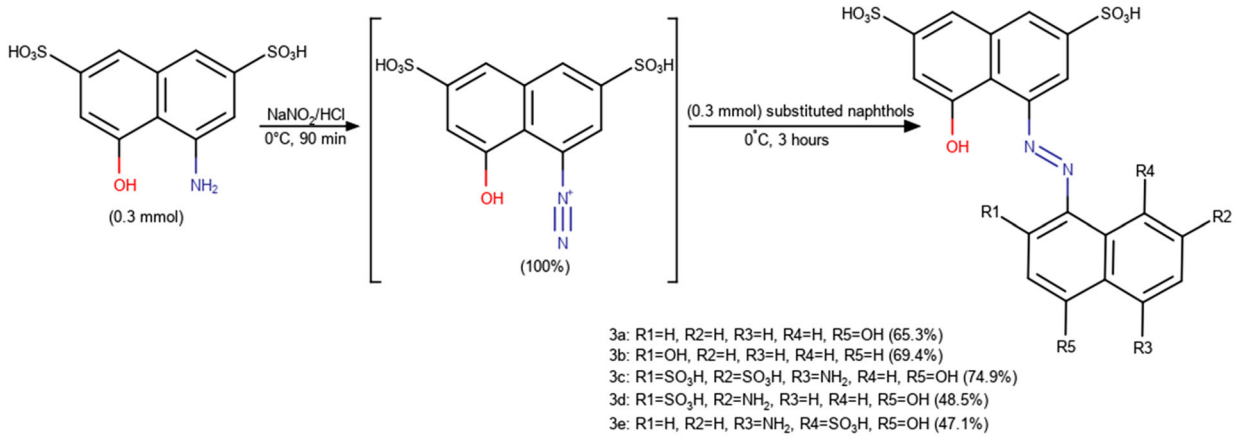

Scheme 1. Synthesis of 8-hydroxy-3,6-disulphonaphthyl azohydroxynaphthalenes (**3a–e**) with yields.

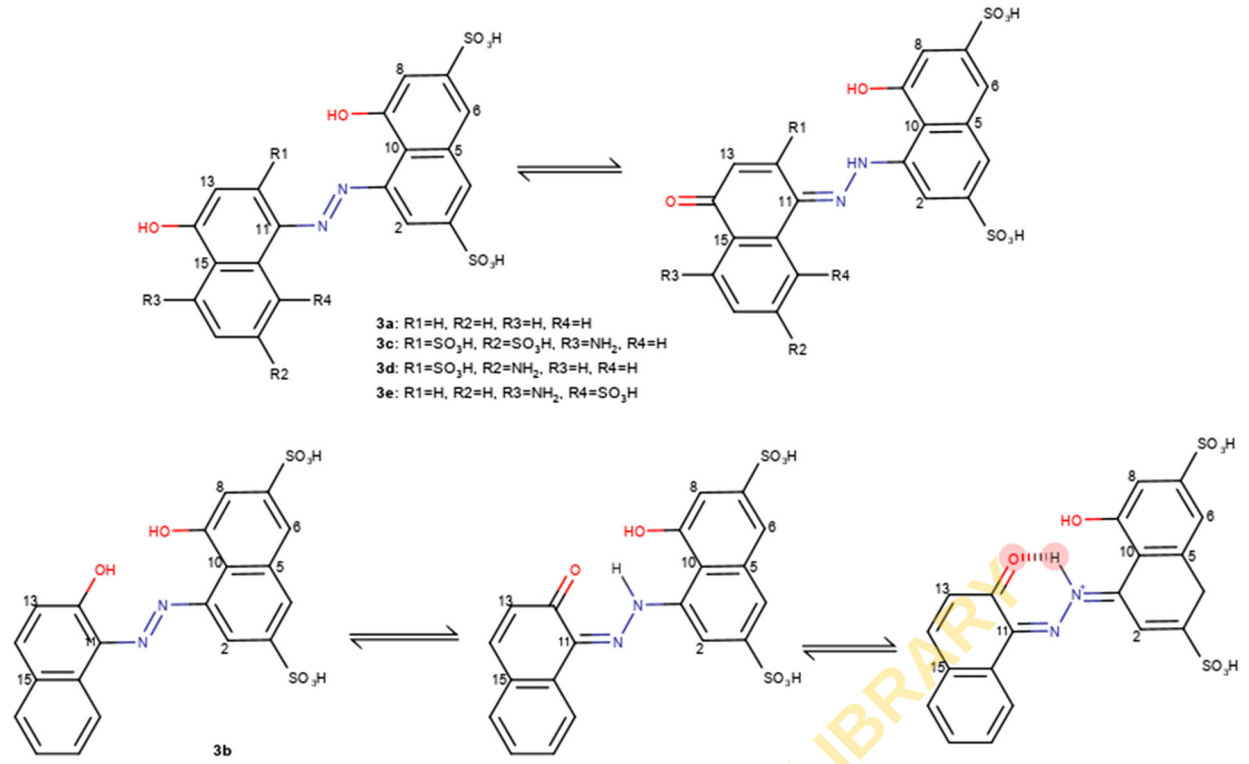

Scheme 2. Azo-hydrazone tautomerism of **3a–e**.

Table 4. Multiple linear regression analysis of the KAT equations for molar transition energies of the dye probes.

Compound	$A_\circ$	A	b	p	F	r^2
3a	63.43			−13.60	31.49	0.76
3b	56.05			−2.47	9.55	0.49
3c	59.16			−8.65	4.85	0.33
3d	64.97			−9.01	22.66	0.70
3e	54.06			−3.65	6.66	0.39

magnitude of the solvent acidity (α), basicity (β) and polarizability (π^*) respectively to the regression model. The Kamlet–Taft parameters with the highest contributions to molar transition energies of the dyes are depicted in Table 4.

A single parametric equation containing solvent polarity produced the best fit for the molar transition energies of the five dye compounds. An inverse relationship between the solvent polarity and the molar transition energy was observed for the compounds. Expectedly, the contribution of solvent polarity to the observed spectral patterns was least with **3b**. This is consistent with the explanation that the intramolecular rearrangement of its hydrazone preclude interaction with solvents.

4. Conclusion

A new series of five tetracyclic azo dyes containing varying types and number of water-solubilizing groups have been synthesized and characterized using UV–visible, IR, NMR and mass spectral analyses. The solvatochromic properties of the compounds in organic solvents have also been elucidated. The compounds could find useful applications as solvatochromic probes, food and drug additives.

Funding

This work was supported by the Consortium for Advanced Research Training in Africa (CARTA) and the University of Ibadan TETFund Academic Staff Training and Development grant. CARTA is funded by the Carnegie Corporation of New York (Grant No–B 8606.R02), Sida (Grant No:54100113), the DELTAS Africa Initiative (Grant No: 107768/Z/15/Z) and Deutscher Akademischer Austauschdienst (DAAD).

Acknowledgement

The authors gratefully acknowledge Dr Tapas Sarkar of the Indian Institute of Chemical Biology and Professor Ghatum Basu of Bose Institute, Kolkata, for their assistance with the NMR and mass spectral analyses.

Disclosure statement

No potential conflict of interest was reported by the author(s).

ORCID

Olusegun E. THOMAS http://orcid.org/0000-0001-8519-2125
Olajire A. ADEGOKE http://orcid.org/0000-0002-8623-3635

References

[1] Selvaraj V, Karthika TS, Mansiya C, et al. An over review on recently developed techniques, mechanisms and intermediate involved in the advanced azo dye degradation for industrial applications. J Mol Struct. 2021;1224:129195.

[2] Chung K-T. Azo dyes and human health: A review. J Environ Sci Heal Part C. 2016;34:233–261.

[3] Chen H. Recent advances in Azo Dye degrading enzyme research. Curr Protein Pept Sci. 2006;7:101–111.

[4] Wojciechowski K, Szadowski J. Effect of the sulphonic group position on the properties of monoazo dyes. Dye Pigment. 2000;44:137–147.

[5] Thomas OE, Adegoke OA, Kazeem AF, et al. Preferential solvation of mordant black and solochrome dark Blue in mixed solvent systems. Prog Chem Biochem Res. 2019;2:40–52.

[6] International Agency for Research on Cancer. Some aromatic amines, organic dyes and related exposures. Lyon; 2010.

[7] Sheng S, Liu B, Hou X, et al. Aerobic biodegradation characteristic of different water-soluble Azo dyes. Int J Environ Res Public Health. 2018;15:35.

[8] Chen H, Xu H, Heinze TM, et al. Decolorization of water and oil-soluble azo dyes by Lactobacillus acidophilus and Lactobacillus fermentum. J Ind Microbiol Biotechnol. 2009;36:1459–1466.

[9] Muthukumar M, Sargunamani D, Selvakumar N. Statistical analysis of the effect of aromatic, azo and sulphonic acid groups on decolouration of acid dye effluents using advanced oxidation processes. Dye Pigment. 2005;65:151–158.

[10] Liu H, Chen Q, Yu Y, et al. Mater. 2013;263:593–599.

[11] Bae J, Freeman HS. Synthesis and evaluation of non-genotoxic direct dyes. Fibers Polym. 2002;3:140–146.

[12] Wadia DN, Patel PM. J Chem. 2008;5:S987–S996.

[13] Blümel S, Knackmuss H-J, Stolz A. Molecular cloning and characterization of the Gene coding for the Aerobic azoreductase fromXenophilus azovoransKF46F. Appl Environ Microbiol. 2002;68:3948–3955.

[14] Morrison RT, Boyd RN. Organic chemistry, 6th ed. New Jersey: Prentice-Hall; 1992.

[15] Williams DA, Lemke TL. Foye's principles of medicinal chemistry, 6th ed. Philadelphia: Lippincott Williams & Wilkins; 2002.

[16] Golka K, Kopps S, Myslak Z. Carcinogenicity of azo colorants: influence of solubility and bioavailability. Toxicol Lett. 2004;151:203–210.

[17] Thomas OE, Adegoke OA. Toxicity of food colours and additives: A review. African J Pharm Pharmacol. 2015;9:900–914.

[18] Cai J, Li Z, Qiu Y, et al. The syntheses, structures and azo–hydrazone tautomeric studies of three triazole/tetrazole azo dyes. New J Chem. 2016;40:9370–9379.

[19] Gilani AG, Yazdanbakhsh MR, Mahmoodi N, et al. Solvatochromism and dichroism of fluorinated azoquinolin-8-ol dyes in liquid and liquid crystalline solutions. J Mol Liq. 2008;139:72–79.

[20] Visentin LC, Ferreira LC, Bordinhão J, et al. Synthesis, structural and spectroscopic studies of novel azo-containing N,O-bonded complexes in the α-iminoketone and azophenolate forms. J Braz Chem Soc. 2010;21:1187–1194.

[21] Morgan KJ. 409. Infrared spectra and structure of arylazonaphthols. J Chem Soc. 1961: 2151–2159.

[22] Adegoke OA, Idowu SO, Olaniyi AA. Synthesis and spectroscopic characterization of 4-carboxyl-2,6-dinitro phenylazohydroxynaphthalenes. Dye Pigment. 2008;77:111–117.

[23] Rauf MA, Hisaindee S, Saleh N. Spectroscopic studies of keto–enol tautomeric equilibrium of azo dyes. RSC Adv. 2015;5:18097–18110.

[24] Matovic L, Tasic N, Trisovic N, et al. On the azo dyes derived from benzoic and cinnamic acids used as photosensitizersin dye-sensitized solar cells. Turkish J Chem. 2019;43:1183–1203.

[25] Mijin D, Božić B, Ladarević J, Ž. Vitnik, et al. Solvatochromism and quantum mechanical investigation of disazo pyridone dye. Color Technol. 2018;134:478–490.

[26] Kurutos A, Kamounah FS, Dobrikov GM, et al. Azo-hydrazone molecular switches: synthesis and NMR conformational investigation. Magn Reson Chem. 2021;59:1116–1125.

[27] Sharifi S, Nazar MF, Rakhshanizadeh F, et al. Impact of amino acids, organic solvents and surfactants on azo-hydrazone tautomerism in methyl Red: spectral-luminescent and nonlinear optical properties. Opt Quantum Electron. 2020;52:1–8.

[28] Hoseini M, Sazgarnia A, Sharifi S. Effect of environment on protoporphyrin IX: absorbance, fluorescence and Nonlinear optical properties. J Fluoresc. 2019;29:531–540.

[29] Ghanadan H, Hoseini M, Sazgarnia A A, et al. Effect of Ion pairs on nonlinear optical properties of crystal violet: surfactants, nano-droplets, and In vitro culture conditions. J Electron Mater. 2019;48:7417–7426.

[30] Hoseini M, Sharifi S, Sazgarnia A. The influence of anionic, cationic surfactant and AOT/water/heptane reverse micelle on photophysical properties of crocin: compare with RPMI effect. J Fluoresc. 2020;30:665–677.